



Effect of cyclic heat treatment on microstructures and mechanical properties of directionally solidified Ti–46Al–6Nb alloy

Hong-ze FANG, Rui-run CHEN, Getman ANTON, Jing-jie GUO, Hong-sheng DING, Yan-qing SU, Heng-zhi FU

School of Materials Science and Engineering, Harbin Institute of Technology, Harbin 150001, China

Received 11 August 2014; accepted 23 January 2015

Abstract: The Ti–46Al–6Nb (mole fraction, %) ingots that were directionally solidified by cold crucible were cyclic heat treated at 1330 °C in the α phase region. The microstructures and mechanical properties of the ingots before and after heat treatment were investigated. The results show that the large columnar grains are changed into equiaxed grains after heat treatment. The grain size decreases with increasing the cyclic times, which is caused by the recrystallization and the transition from the large grain of small lamellae to the small grain of large lamellae. Four times of cyclic heat treatment refines the grain size from 1.33 mm to 0.59 mm, nevertheless the lamellar spacing increases from 0.71 μm to 1.38 μm . Extending the holding time and increasing the cyclic times of heat treatment eliminate the β -segregation at the grain boundary and the interlamellar. The compression testing shows that the compressive strength of the directionally solidified ingot in the parallel and perpendicular directions are 1385.09 MPa and 1267.79 MPa, respectively, which are improved to 1449.75 MPa and 1527.76 MPa after two and four times of cyclic heat treatment, respectively, while that is 1180.64 MPa for the as-cast sample. The fracture mode of the sample after cyclic heat treatment is quasi-cleavage fracture.

Key words: TiAl alloy; cyclic heat treatment; directional solidification; mechanical properties

1 Introduction

TiAl-based alloys with high Nb content can greatly improve the high temperature mechanical properties and oxidation resistance, which will be applied to aviation and aircraft industry [1–5]. γ -TiAl alloys with Nb content ranging from 4% to 10% (mole fraction) and Al content ranging from 42% to 49% (mole fraction) were extensively researched [6–8]. Because of the fragile nature of TiAl-based alloys, adding high Nb content into them led to worse plasticity at room temperature and hot working performance [9]. In order to solve this problem, LUAN et al [10] studied the mechanical properties of Ti–16Al–12Nb and Ti–16Al–12Nb–3Cr–Mo alloys using the CaO crucible for directional solidification, and pointed out that the fracture type was transgranular fracture in low stress at 600 °C and ductile creep crack was produced at 700 °C. LAPIN et al [11,12] directionally solidified Ti–46Al–8Ta and Ti–46Al–8Nb alloys with Y_2O_3 crucible, and found that Y_2O_3 could increase the oxygen content of the

alloys and then part of Y_2O_3 was shed into the alloys. Therefore, the ceramic crucible will seriously contaminate the alloy and deteriorate its mechanical properties during directional solidification (DS). Cold crucible directional solidification is a newly developed technique to directionally solidify TiAl alloys without contamination [13].

Because of the peritectic solidification and subsequent the solid phase transformation during DS, heat treatment is a necessary process to optimize the microstructure of the DS alloys [14]. Recent researches on heat treatments of cast Ti–45Al–8Nb alloys demonstrated that after heat treatment at 1250 °C for 24 h and 900 °C for 30 min with air cooling (AC), B2 phase can be entirely eliminated from the cast microstructure, both Al-segregation and B2 phase can be removed after heat treatment at 1400 °C for 12 h and 900 °C for 30 min with air cooling [15,16]. In the study of heat treatment of TiAl-based alloys slab solidified directionally with cold crucible, it was found that the cyclic heat treatment at 1150 °C can refine lamellae and improve the mechanical properties compared with the conventional solid solution

treatment [17]. Additionally, the development of a cyclic heat treatment for obtaining microstructures from the cast/hot isostatic pressing (HIP) condition with improved RT-ductility was a further step to apply to higher ductility requirements [18]. The characterization of final heat-treated TiAl–Nb–Mo (TNM) alloys on the nano-scale regarding lamellar spacing within the α_2/γ -colonies and the existence of ω -phase domains with $B8_2$ structure within the β_0 -phase were reported in Refs. [19,20]. Generally, the cast and heat-treated TNM microstructures possess the potential to concur with forged and heat-treated TNM material, especially when high strength and creep resistance are required and the demand on RT-fracture elongation is moderate [21].

Block type transformation will happen when the TiAl alloy cools rapidly from α phase region, which will influence the phase composition. Discontinuous coarsening (DC) is a course that the smaller grains nucleate and grow on the original lamellar, and the lamellae spacing in the new small grains becomes bigger. During solidification, the higher the cooling speed is, the smaller the original grains are. Many researches of heat treatment were carried out on the equiaxed TiAl alloys, but the references of heat treatment on directional solidification are very few. In this study, directionally solidified Ti–46Al–6Nb alloys were heat treated in α phase region at different holding time and cyclic times. The effects of cyclic heat treatment on the microstructures, β -segregation and mechanical properties were studied, and the mechanisms of which were discussed.

2 Experimental

The investigated Ti–46Al–6Nb ingot was prepared by cold crucible directional solidification [22]. The ingot was cut in half longitudinally, and then polished and etched. The macrostructure of the ingot is shown in Fig. 1. The average grain size was calculated by intersection method. The sample size for heat treatment is 8 mm × 6 mm × 12 mm. These samples were sealed in quartz tubes that were filled with argon gas. The type of furnace for heat treatment is GSL-1600. These samples were heated to 1330 °C slowly, held at this temperature for some time and then cooled in air, the details of heat treatment are listed in Table 1. The microstructures and the phases of the samples were examined by an Olympus GX71 optical microscope (OM) and an Quanta 200F scanning electron microscope (SEM). The samples with the size of $d3$ mm × 4.5 mm were used for compressive testing which was operated on an Instron 5960 Dual Column Tabletop Universal Testing System. For directionally solidified samples, the samples were cut in two directions that were the parallel direction (the

columnar grain direction parallel to the axis of the sample, LS) and the perpendicular direction (the columnar grain direction perpendicular to the axis of the sample, TS).



Fig. 1 Macrostructure of directionally solidified ingot

Table 1 Parameters of heat treatment

Heat treatment	Parameter
HT1	(1330 °C for 2 h, AC)+(1330 °C for 10 min, AC)
HT2	(1330 °C for 10 min, AC)+(1330 °C for 10 min, AC)
HT3	1330 °C for 10 min, AC (repeat four times)

3 Results and discussion

3.1 Macrostructures of samples

The macrostructures of the as-cast, the directionally solidified samples before and after heat treatment are shown in Fig. 2. The average grain size of these samples is shown in Table 2. It can be seen that the macrostructure of the as-cast sample is equiaxed and the average grain size is 1.42 mm (Fig. 2(a)). The directionally solidified sample is columnar and the average width is about 1.09 mm (Fig. 2(b)). The heat treatments HT1–HT3 changed the crystal morphology from columnar to equiaxed. There are big equiaxed grains after HT1 (Fig. 2(c)). Compared with the directionally solidified sample, for the heat treated samples, the number of the equiaxed grains increases obviously and the columnar crystal disappeared. Contrasting HT2 with HT1, the condition of 1330 °C for 2 h increases the grain size. Comparing HT3 with HT2, increasing the times of cyclic heat treatment can reduce the average grain size. So four times of cyclic heat treatment with a holding time of 10 min (Fig. 2(e)) not only changes the columnar crystal into equiaxed grains, but also refines the grain size. The relationship between

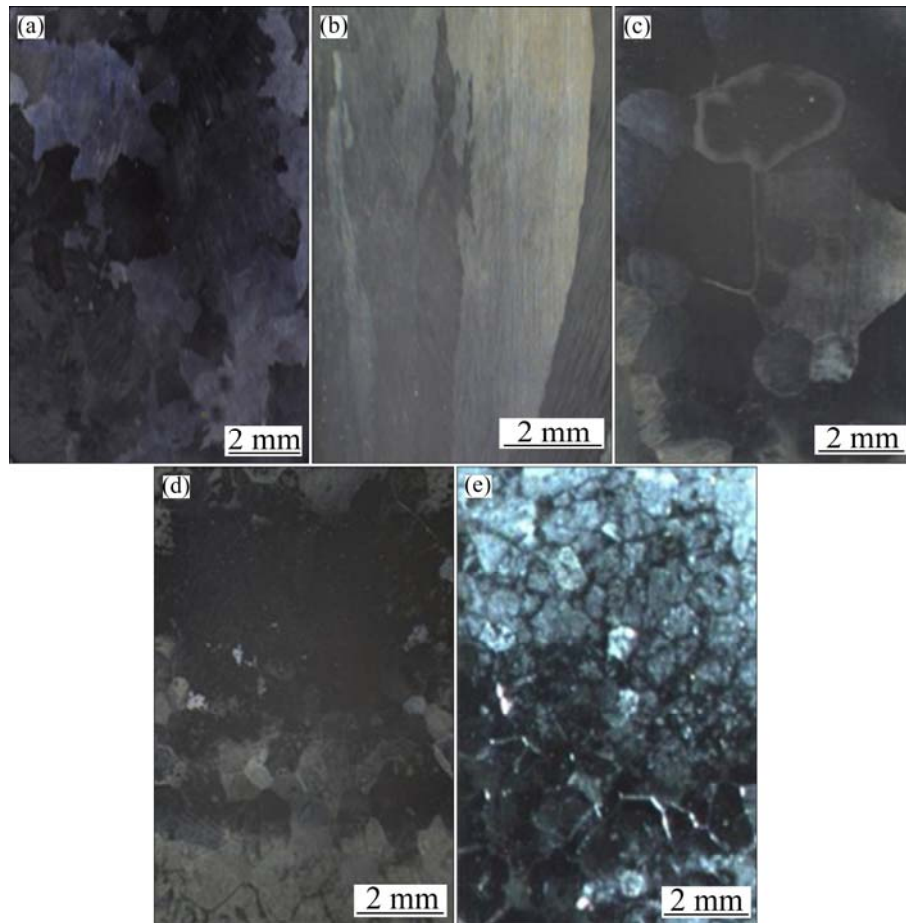


Fig. 2 Macrostructures of samples before and after heat treatment: (a) As-cast; (b) Directionally solidified sample; (c) HT1; (d) HT2; (e) HT3

Table 2 Average grain size of samples (mm)

As-cast	DS	HT1	HT2	HT3
1.42	Columnar	1.33	0.73	0.59

the average grain size and the holding time obeys the exponential rule [23]. In polycrystalline materials, the exponential law can be expressed as

$$D=c_1 \times t^n \quad (1)$$

where D is the average grain size, t is the holding time, and n is the factor of grain growth. That is to say, the extension of the time can increase the average grain size. If the anisotropy and the interfacial energy are not considered, the crystal nucleus will form on the inter-crystalline that should be double lens shape [24] (Fig. 3). Since one γ crystal cell has four $\{111\}$ equivalent surfaces, the γ -TiAl based alloy can precipitate α lamellae with four different orientations at every time of cyclic heat treatment. It can satisfy the orientation relationship $((0001)_\alpha // (111)_\gamma)$ of α_2 and γ lamellae. The TiAl based alloy can get a better grain-refined effect when it is cooled from α phase to two phases ($\alpha+\gamma$) region after cyclic heat treatment. Due

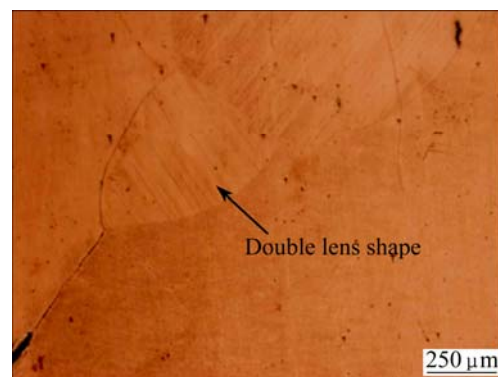


Fig. 3 Microstructure of double lens of alloy shape after HT1

to the discontinuous coarsening, the refining is achieved by the transition from the large grain of small lamellae to the small grain of large lamellae.

3.2 Microstructures of samples before and after heat treatment

Figure 4 shows the microstructures of the as-cast and the directionally solidified samples. The average lamellar spacing of the directionally solidified alloy is shown in Table 3. The white lamellae is α_2 phase and the

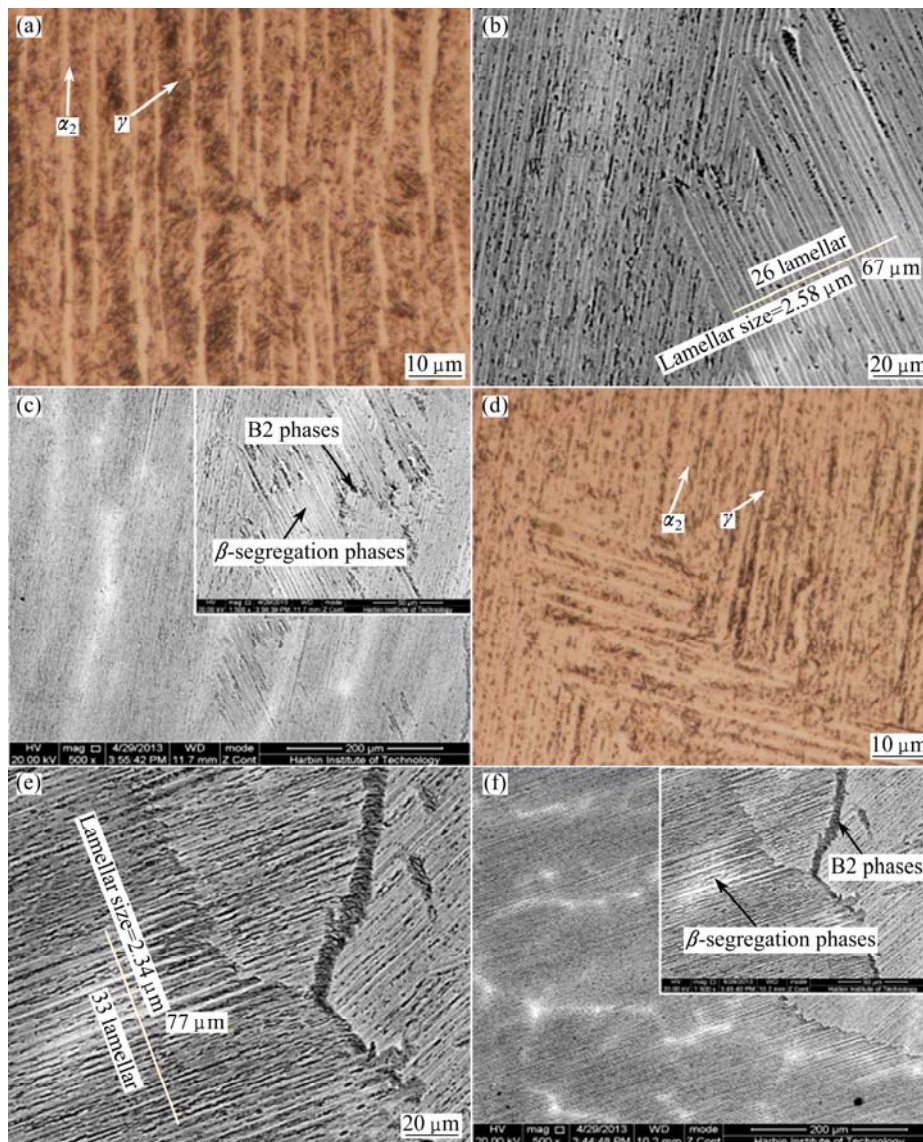


Fig. 4 Microstructures of samples without heat treatment: (a, b, c) Directionally solidified sample; (d, e, f) As-cast sample

Table 3 Average lamellar spacing of samples (μm)

As-cast	DS	HT1	HT2	HT3
2.34	2.58	1.07	0.71	1.38

black lamellae is γ phase in Figs. 4(a) and (d). Contrasting Figs. 4(a) with (d), the lamellar direction of the growth in the directionally solidified samples is almost similar. Comparing Figs. 4(b) and (e), the lamellar spacing increases from 2.34 μm for the as-cast to 2.58 μm for the DS sample. It can be seen that there are lots of β -segregation phases (Fig. 4(f)) that have the same direction as lamellar growth in the DS sample (Fig. 4(c)).

The microstructures of the directionally solidified samples after HT1–HT3 are shown in Fig. 5. Comparing Fig. 4 with Fig. 5, it is shown that the columnar crystal edge of the original directionally solidified samples is uneven, while the lamellar edge of the equiaxed grain is

even. This is because of the change of the lamellar direction in the new crystals resulting from the recrystallization. After HT1, the average lamellar spacing is approximately 1.07 μm . Comparing with the DS sample, the spacing of the heat-treated ones is significantly reduced, especially the lamellar spacing is 0.71 μm after HT2. Contrasting with the as-cast sample, it is shown that there is no big B2 phase in the microstructures of the sample after HT1–HT3. In Fig. 5(b), some small white dots are the β -segregation phases. It is shown that under the heat treatment at 1330 $^{\circ}\text{C}$ for 2 h, the β -segregation phase can be reduced effectively. Figure 5(e) shows that the average lamellar spacing of the directionally solidified sample is 1.38 μm after HT3. Comparing with HT2, increasing the cyclic heat treatment times will increase the lamellar spacing and decrease the segregation. A feather-shaped γ_f phase is shown in HT3 sample. The fast cooling speed is

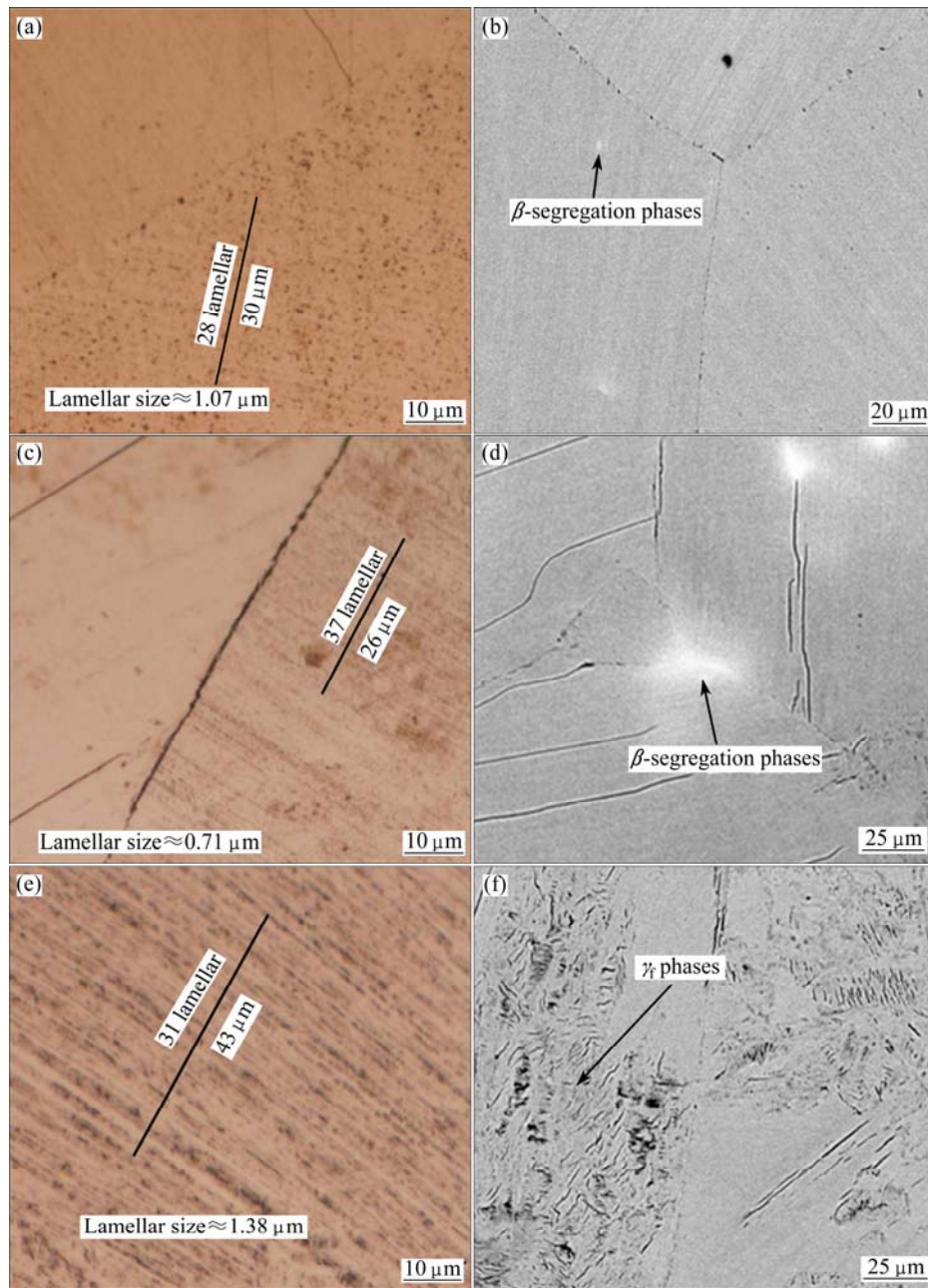


Fig. 5 Microstructures of samples after heat treatment: (a, b) HT1; (c, d) HT2; (e, f) HT3

beneficial to forming γ_m block phase during cooling from α phase region. This γ_m phase has high density of flaws, such as stacking faults, dislocations and antiphase domain boundaries. These existing flaws are favorable for α phase nucleation in γ_m phase. But with the decrease of cooling speed, the block γ_m phase will reduce and the γ_f phase will increase. This feather-shaped γ_f phase, which is hard for α phase forming in it [25], has flaws less than those of the γ_m phase. Air cooling method is adopted in this experiment, and the speed is relatively slow, therefore the γ_f phase will form and the α phase nucleation will be less. More γ_f phases are found in HT3 samples and none is found in HT1 and HT2 samples.

Nb serves as the stable element of β phase [26]. Due

to the extremely low diffusion rate, Nb element forms solid solution that exists in inter-crystalline of TiAl alloy. This will increase the constitutional supercooling degree [27]. Comparing Fig. 4(c) with Figs. 5(b), (d) and (f), it is found that the amount of β -segregation phase significantly decreases after long holding time or four times of cyclic heat treatment. As shown in Fig. 6, during solidification, a transformation pathway is: $L \rightarrow L + \beta \rightarrow \beta \rightarrow \alpha + \beta \rightarrow \alpha + \beta_r \rightarrow \alpha + \gamma + \beta_r \rightarrow \text{lamellae } (\alpha_2 + \gamma) + \gamma + \beta_r$. The β_r phase is the residual β phase when the alloy cools down to room temperature. Because the β phase contains abundant Ti element and less Al element, the γ phase has more Al element and less Ti element, when the β phase dissolves in the first heating process, it will absorb Al

element and expel Ti element from the surrounding γ phase and $(\alpha_2+\gamma)$ lamellar colony. The β phase will not transform into α phase until reaching the component of α phase. The reason is that the same content of Nb in the two phases is easy to satisfy the component fluctuation and has smaller driving force of phase transformation.

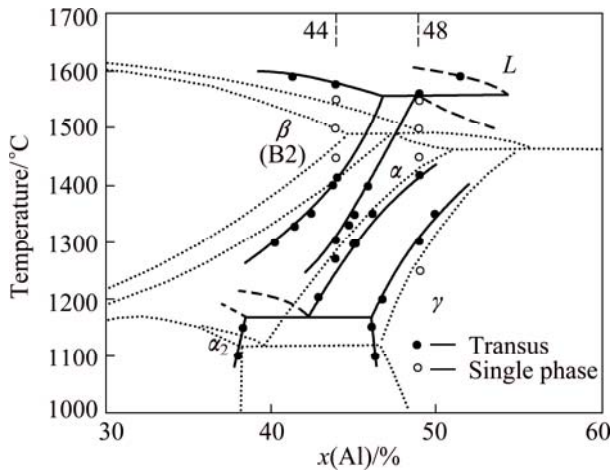


Fig. 6 Phase diagram of TiAl alloy with 8% Nb [21]

Comparing HT2 with HT3, the lamellar spacing of the newly-formed DC grain is larger than that of the original grain. DC will happen in the grain boundary and the lamellar colony, and the lamellar direction will change during the first time heat treatment of HT3. In the next heat treatment, this DC continuously and simultaneously happens in the primary lamellae and the newly-formed DC lamellae. The driving force of phase transformation in DC and the interfacial energy obeys the thermodynamic relation that can be expressed as [28]

$$\Delta F_v = 2\sigma_{\alpha_2/\gamma}[1/\lambda_2 - 1/\lambda_1]V_m \quad (2)$$

where ΔF_v is the driving force of phase transformation, $2\sigma_{\alpha_2/\gamma}$ represents the interfacial energy of α_2 and γ , λ_1 and λ_2 are the lamellar spacing before and after DC, respectively, and V_m is the molar volume.

From the thermodynamic relation between the driving force and the lamellar spacing, it can be seen that DC will occur on the smaller spacing lamellae. With the processing of HT3, the volume fraction of DC lamellae increases until all of the original small spacing lamellae are replaced by the large spacing DC lamellae. The lamellar spacing increases from $0.71 \mu\text{m}$ to $1.38 \mu\text{m}$ after HT3. In the process of HT3, the crystal morphology changed from columnar to equiaxed. Due to the effect of phase change, the cyclic heat treatment finally refines the grain. In air cooling process, not only the DC occurs, but also the feather-shaped γ_f phase forms. Finally the degree of refining grain is the best and the lamellar spacing is larger after HT3.

3.3 Compressive properties

The compressive strength of the as-cast, directionally solidified and heat-treated samples is shown in Fig. 7. It can be seen that the compressive strength of the two directions of DS samples are higher than that of the as-cast samples. The compressive strength of DS sample in the parallel direction (1385.09 MPa) is higher than that in the perpendicular direction (1267.79 MPa). This is because the microstructures of the two directions in the DS sample are quite different. After HT1–HT3, the crystal transforms from columnar to equiaxed, so that the effect of the direction is diminished. After HT1, the compressive strength decreases to 1213.72 MPa. This is because during the holding time of 2 h at $1330 \text{ }^\circ\text{C}$, the equiaxed grain has bigger grain size. Contrasting HT2 with HT3, increasing the times of cyclic heat treatment, the compressive strength increases to 1527.76 MPa after HT3. This is because the cyclic heat treatment refines the grain size, and the fine grain effectively prevents the dislocation movement and improves the compressive strength. After HT3, the lamellar spacing increases, but the degree of grain refinement plays a major role on the compressive strength. Comparing HT3 with the as-cast sample, the compressive strength of the alloy increases by 29.4%.

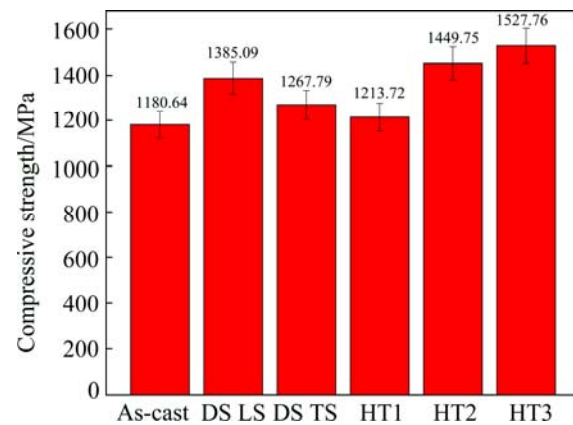


Fig. 7 Compressive strength of samples

3.4 Fracture morphologies

The fracture morphologies of the samples before and after heat treatment is shown in Fig. 8. There is no obvious plastic deformation at the fracture position. All of the samples are brittle fracture. The fracture morphologies have significant large platform, so they are shear fracture in Figs. 8(a) and (d). There are many cleavage facets with strong luminescence in Figs. 8(b) and (c). Mutually parallel cleavage platform in varied height joins into forming the river pattern, finally forming the relatively typical cleavage fracture. The fracture mode is quasi-cleavage fracture in Figs. 8(e) and (f). Especially in Fig. 8(f), because of the smaller grain size, the dimple with parabolic shape is more obvious

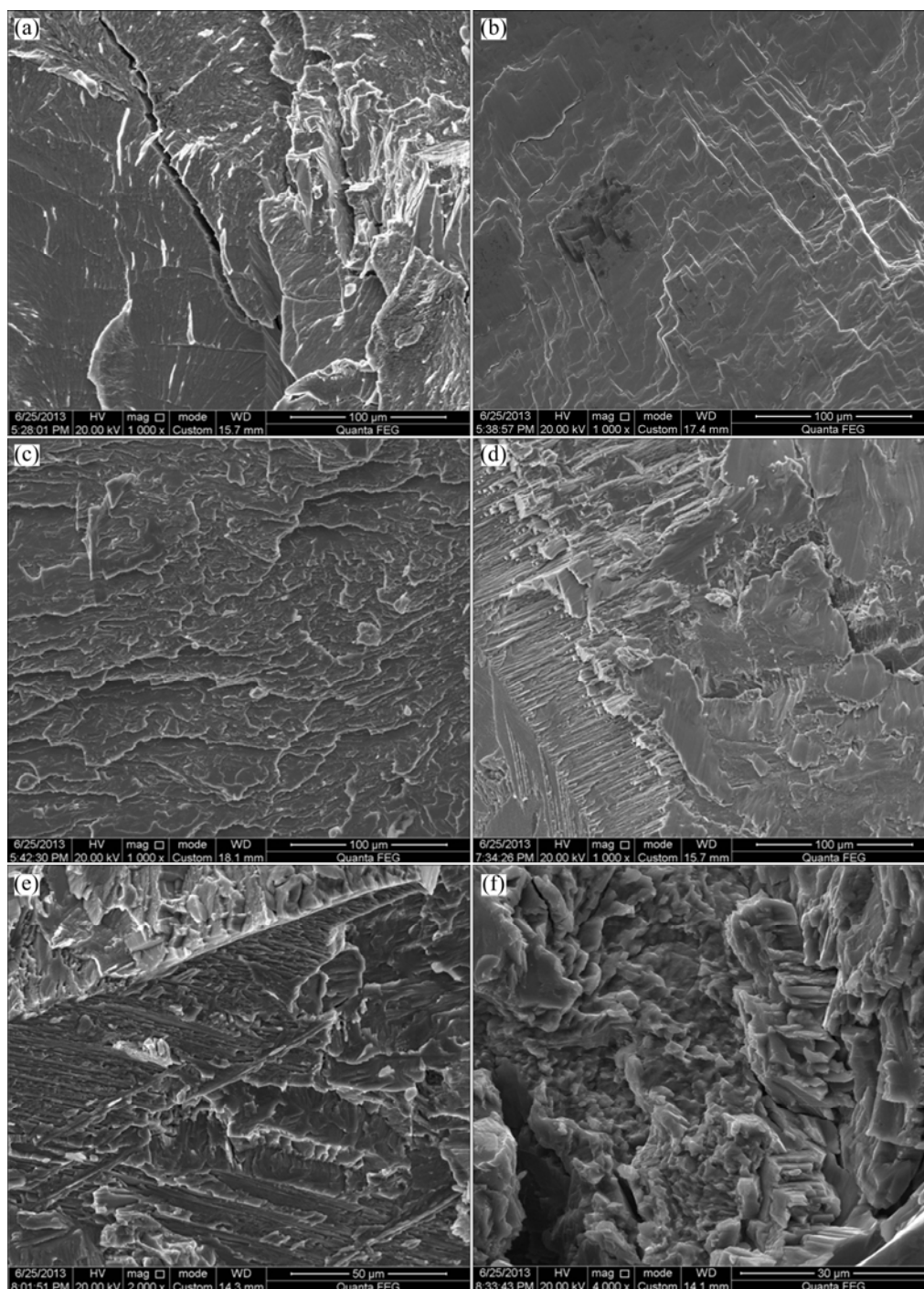


Fig. 8 Fracture morphologies of samples: (a) As-cast; (b) LS of DS sample; (c) TS of DS sample; (d) HT1; (e) HT2; (f) HT3

than that in Fig. 8(e). It explains the compressive property being improved after HT3.

In a word, the grain size plays a major role on the compressive strength and fracture morphologies of the samples. The amount of β -segregation phase obviously decreases after HT1. But because of the big grain size, the compressive strength and the fracture morphology are the same as those of the as-cast sample. The grain size becomes smaller and the β -segregation phase reduces after four times of cyclic heat treatment, so the

compressive strength is the best and the fracture morphology forms the feature of dimple.

4 Conclusions

1) The macrostructure of the as-cast sample is equiaxed and the average grain size is 1.37 mm, while the directionally solidified sample is columnar and the average width is 1.09 mm. Heat treatment changes the crystal morphology from columnar to equiaxed. Four

times of cyclic heat treatment can refine the grain size from 1.33 mm to 0.59 mm. The refining is achieved by the transition from the large grain of small lamellae to the small grain of large lamellae during the discontinuous coarsening.

2) The lamellar spacing increases from 2.34 μm for the as-cast sample to 2.58 μm for the DS sample. The average lamellar spacing is approximately 1.07 μm after HT1 and 0.71 μm after HT2, which increases to 1.38 μm after HT3. DC will occur on the smaller spacing lamellae. The volume fraction of DC lamellae increases until all of the original small spacing lamellae are replaced by the large spacing DC lamellae. The β -segregation phase significantly decreases after holding time of 2 h at 1330 $^{\circ}\text{C}$ or four times of cyclic heat treatment. The feather-shaped γ_f phase forms after heat treatment.

3) The compressive strength of the as-cast sample is 1180.64 MPa, and that of the DS samples is 1385.09 MPa in the parallel direction and 1267.79 MPa in the perpendicular direction. After HT1, as a result of the grain size increasing, the compressive strength of the alloy is 1213.72 MPa. After four times of cyclic heat treatment, the compressive strength is about 1527.76 MPa, and the refined crystalline strengthening plays a major role. The fracture mode of the DS sample is cleavage fracture, and that is shear fracture after HT1 and quasi-cleavage fracture after HT2 and HT3.

References

- [1] CHEN Rui-run, DING Hong-sheng, YANG Jie-ren, HUANG Feng, SU Yan-qing, GUO Jing-jie, FU Heng-zhi. Temperature field calculation on cold crucible continuous melting and directional solidifying Ti50Al alloys [J]. Transactions of Nonferrous Metals Society of China, 2012, 22: 647–653.
- [2] QIU Cong-zhang, LIU Yong, HUANG Lan, LIU Bin, ZHANG Wei, HE Yue-hui, HUANG Bo-yun. Tuning mechanical properties for β (B2)-containing TiAl intermetallics [J]. Transactions of Nonferrous Metals Society of China, 2012, 22: 2593–2603.
- [3] WANG Yan, LIU Yong, YANG Guang-yu, LI Hui-zhong, TANG Bei. Microstructure of cast γ -TiAl based alloy solidified from β phase region [J]. Transactions of Nonferrous Metals Society of China, 2011, 21: 215–222.
- [4] GAITZENAUER A, MÜLLER M, CLEMENS H, VOIGT P, HEMPEL R, MAYER S. Eigenschaftsoptimiertes warmumformen einer intermetallischen titanaluminid-legierung [J]. BHM Berg-Und Hüttenmännische Monatshefte, 2012, 157: 319–322.
- [5] CLEMENS H, MAYER S. Design, processing, microstructure, properties, and applications of advanced intermetallic TiAl alloys [J]. Advanced Engineering Materials, 2013, 15: 191–215.
- [6] LU Bin, HUANG Lan, LIU Yong, LIANG Xiao-peng, LIU Bin, HE Yue-hui, LI Hui-zhong. Evolution of lamellar structure in Ti-47Al-2Nb-2Cr-0.2W alloy sheet [J]. Transactions of Nonferrous Metals Society of China, 2013, 23: 1293–1298.
- [7] LIN J P, XU X J, WANG Y L. High temperature deformation behaviors of a high Nb containing TiAl alloy [J]. Intermetallics, 2007, 15: 668–674.
- [8] STARK A, BARTELS A, CLEMENS H. On the formation of ordered χ phase in high Nb containing γ -TiAl based alloy [J]. Advanced Engineering Materials, 2008, 10: 929–934.
- [9] DING Xian-fei, LIN Jun-pin, ZHANG Lai-qi, WANG Yan-li, YE Feng, CHEN Guo-liang. Structure of directional solidification of high niobium [J]. Journal of Materials Engineering, 2009 (S1): 258–262. (in Chinese)
- [10] LUAN Q D, DUAN Q Q, WANG X G, LIU J, PENG L M. Tensile properties and high temperature creep behavior of micro-alloyed Ti-Ti3Al-Nb alloys by directional solidification [J]. Materials Science and Engineering A, 2010, 27: 4484–4496.
- [11] LAPIN J, GABALCOVÁ Z, PELACHOVÁ T. Effect of Y_2O_3 crucible on contamination of directionally solidified intermetallic Ti-46Al-8Nb alloy [J]. Intermetallics, 2011, 19: 396–403.
- [12] LAPIN J, GABALCOVÁ Z. Solidification behaviour of TiAl-based alloys studied by directional solidification technique [J]. Intermetallics, 2011, 19: 797–804.
- [13] DING Hong-sheng, GUO Jing-jie, CHEN Rui-run, FU Heng-zhi. Development of directional solidification technology based on electromagnetic cold crucible to prepare TiAl intermetallics [J]. Rare Metals Letters, 2010, 29: 14–23. (in Chinese)
- [14] DING Xian-fei, LIN Jun-pin, ZHANG Lai-qi. Effects of heat treatment on microstructure of directionally solidified Ti-45Al-8Nb-(W,B,Y) alloy [J]. Transactions of Nonferrous Metals Society of China, 2011, 21: 26–31.
- [15] XU Z F, XU X J, LIN J P. Effect of heat treatment on S-segregation of microstructure for as-cast high Nb containing TiAl alloy [J]. Journal of Aeronautical Materials, 2007, 27: 28–32.
- [16] XU Z F, XU X J, LIN J P. Elimination of β phase segregation in as-cast high Nb containing TiAl alloy by heat treatment [J]. Journal of Materials Engineering, 2007, 9: 42–46.
- [17] DING Hong-sheng, LIAO Bo-chao, CHEN Rui-run, NIE Ge, GUO Jing-jie, FU Heng-zhi. Heat treatment on TiAl-based alloy slabs solidified directionally with cold crucible [J]. Transactions of Materials and Heat Treatment, 2010, 1: 7–12. (in Chinese)
- [18] SCHWAIGHOFER E, SCHLOFFER M, SCHMOELZER T, MAYER S, LINDEMANN J, GUETHER V, KLOSE J, CLEMENS H. Influence of heat treatments on the microstructure of a multi-phase titanium aluminide alloy [J]. Practical Metallography, 2012, 49: 124–137.
- [19] CHA L, CLEMENS H, DEHM G. Microstructure evolution and mechanical properties of an intermetallic Ti-43.5Al-4Nb-1Mo-0.1B alloy after ageing below the eutectoid temperature [J]. International Journal of Materials Research, 2011, 102: 703–708.
- [20] SCHLOFFER M, IQBAL F, GABRISCH H, SCHWAIGHOFER E, SCHIMANSKY F P, MAYER S, STARK A, LIPPMANN T, GÖKEN M, PYCZAK F, CLEMENS H. Microstructure development and hardness of a powder metallurgical multi phase γ -TiAl based alloy [J]. Intermetallics, 2012, 22: 231–240.
- [21] SCHWAIGHOFER E, CLEMENS H, MAYER S, LINDEMANN J, KLOSE J, SMARSLY W, GÜTHER V. Microstructural design and mechanical properties of a cast and heat-treated intermetallic multi-phase γ -TiAl based alloy [J]. Intermetallics, 2014, 44: 128–140.
- [22] YANG J R, CHEN R R, DING H S, GUO J J. Erratum: Flow field and its effect on microstructure in cold crucible directional solidification of Nb containing TiAl alloy [J]. Journal of Materials Processing Technology, 2013, 213: 1355–1363.
- [23] SONG Yang, LI Hui-zhong, LIANG Xiao-peng, LIU Yong, ZHANG Dan-yang, WEI Zhong-wei. Effect of heat treatment on microstructure of HIP Ti-47Al-2Cr-2b-0.2W alloy [J]. Materials Science and Engineering of Powder Metallurgy, 2013, 18: 706–712. (in Chinese)
- [24] PENG Chao-qun, SHU Chang, HUANG Bo-yun. Formation of fine fully-lamellar microstructure of TiAl-based alloy in rapid heating cyclic heat treatment process [J]. Nonferrous Metals, 2003, 55: 8–12.

- (in Chinese)
- [25] PENG Chao-qun, HUANG Bo-yun, HE Yue-hui. Study on refining of TiAl-based alloy by rapid heating cyclic heat treatment [J]. Rare Metal Materials and Engineering, 2002, 31: 192–196. (in Chinese)
- [26] HU Rui, LIU Yi, ZHANG Tie-bang, KOU Hong-chao, LI Jin-shun. Phase selection and the solidification characteristics of TiAl base alloys in the nonequilibrium solidification [J]. Acta Metallurgica Sinica, 2013, 49: 1295–1302. (in Chinese)
- [27] LI Jian-bo, LIU Yong, WANG Yan, LIU Bin, LU Bin, LIANG Xiao-peng, LIU Yan-bin. Eliminating of β (B2) phase of as-cast TiAl based alloy by heat treatment [J]. Materials Science and Engineering of Powder Metallurgy, 2012, 17: 687–693. (in Chinese)
- [28] XIAO Dai-hong, HUANG Bo-yun. Grain refinement of Ti–46Al–2Nb–2Cr alloy by cyclic heat treatment [J]. Heat Treatment of Metals, 2008, 33: 62–65. (in Chinese)

循环热处理对定向凝固 Ti–46Al–6Nb 合金组织和力学性能的影响

方虹泽, 陈瑞润, Anton GETMAN, 郭景杰, 丁宏升, 苏彦庆, 傅恒志

哈尔滨工业大学 材料科学与工程学院, 哈尔滨 150001

摘要: 利用冷坩埚定向凝固技术制备 Ti–46Al–6Nb (摩尔分数, %) 合金, 然后对定向凝固铸锭进行热处理, 热处理温度为 1330 °C, 热处理区间在 α 相单相区。研究热处理前后铸锭显微组织和力学性能的变化。结果表明: 铸锭经过热处理后, 大的柱状晶转变为等轴晶。随着热处理循环次数的增加, 晶粒尺寸减小, 这是由于发生了再结晶和小片层的大晶粒与大片层的小晶粒之间的转变。四次循环热处理能够有效地细化晶粒尺寸, 使晶粒尺寸从 1.33 mm 降低到 0.59 mm, 然而片层间距从 0.71 μm 增加到 1.38 μm 。延长保温时间和增加热处理循环次数能够消除晶粒间和片层间的 β 偏析相。压缩实验结果表明, 对定向凝固铸锭, 平行于柱状晶生长方向的压缩强度为 1385.09 MPa, 垂直于柱状晶生长方向的压缩强度为 1267.79 MPa; 铸造试样的压缩强度为 1180.64 MPa, 经热处理循环两次后压缩强度提高到 1449.75 MPa, 热处理循环 4 次后压缩强度提高到 1527.76 MPa。循环热处理后, 合金试样的断裂方式为准解理断裂。

关键词: TiAl 合金; 循环热处理; 定向凝固; 力学性能

(Edited by Mu-lan QIN)